Department of Applyied Physics

Topological superconductivity in magnetic adatom lattices

Joel Röntynen

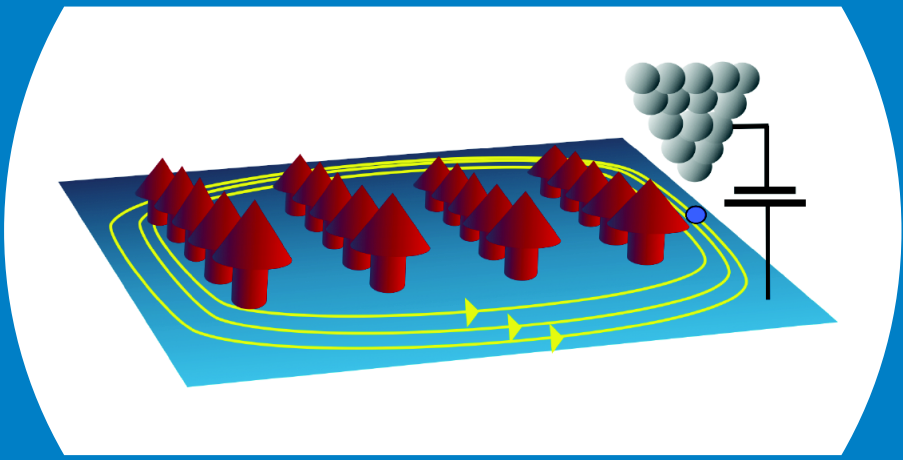

Aalto University

DOCTORAL DISSERTATIONS

Aalto University publication series
DOCTORAL DISSERTATIONS 111/2016

Topological superconductivity in magnetic adatom lattices

Joel Röntynen

A doctoral dissertation completed for the degree of Doctor of Science (Technology) to be defended, with the permission of the Aalto University School of Science, at a public examination held at the lecture hall TUAS/1017 of the school on 17 June 2016 at 12.

Aalto University
School of Science
Department of Applied Physics

Supervising professor
Pertti Hakonen

Thesis advisor
Teemu Ojanen

Preliminary examiners
Patrik Recher, Technische Universität Braunschweig, Germany
Timo Hyart, University of Jyväskylä, Finland

Opponent
Björn Trauzettel, Würzburg University, Germany

Aalto University publication series
DOCTORAL DISSERTATIONS 111/2016

ISBN 978-952-60-6851-0 (printed)
ISBN 978-952-60-6852-7 (pdf)
ISSN-L 1799-4934
ISSN 1799-4934 (printed)
ISSN 1799-4942 (pdf)
http://urn.fi/URN:ISBN:978-952-60-6852-7

Unigrafia Oy
Helsinki 2016

Finland

441 697
Printed matter

Aalto University

Abstract

Aalto University, P.O. Box 11000, FI-00076 Aalto www.aalto.fi

Author
Joel Röntynen

Name of the doctoral dissertation
Topological superconductivity on magnetic adatom lattices

Publisher School of Science

Unit Department of Applied Physics

Series Aalto University publication series DOCTORAL DISSERTATIONS 111/2016

Field of research Theoretical Condensed Matter Physics

Manuscript submitted 3 February 2016 **Date of the defence** 17 June 2016

Permission to publish granted (date) 16 May 2016 **Language** English

☐ **Monograph** ☒ **Article dissertation** ☐ **Essay dissertation**

Abstract

Topological matter has emerged as one of the most prominent research fronts in condensed matter physics over the past three decades. The discovery of the role of topology in materials has shaped our fundamental understanding of how the constituents of matter organize themselves to produce various phases. Topology in these systems manifests as boundary states and exotic quasiparticles, whose intriguing properties are anticipated to facilitate various technological applications.

In this thesis I have contributed to the search for topological superconductivity, which is expected to support localized, particle-like excitations called Majorana bound states. Majorana bound states break the dichotomy of bosons and fermions by obeying non-Abelian exchange statistics. Hence a Majorana bound state would be a manifestation of a fundamentally new type of physics. Furthermore, Majorana braiding is envisioned to be utilized in topologically protected quantum computing, which could revolutionize the future of computing. The experimental discovery of Majorana bound states is an outstanding goal in condensed matter physics at the moment.

The systems investigated in this thesis consists of magnetic adsorbed atoms (adatoms) deposited on top of a conventional superconductor. In publications I and II we investigated the appearance of Majorana bound states in adatom chains. The main result in publication I is that coupled chains are more likely to exhibit Majorana bound states than uncoupled chains. In publication II we showed that a supercurrent can be used to control the topological phase, which could be helpful for the manipulation of Majorana bound states.

In publications III and IV we showed that two-dimensional adatom structures support a generalization of p_x+ip_y superconductivity, making it an interesting addition to the list of materials with unconventional superconductivity. The complex, mosaic-like structure of the topological phase diagram is remarkably rich due to long-range electron hopping. The number of propagating Majorana modes at the boundary is given by a topological invariant called a Chern number. We predicted that for typical experimentally available materials this number can be much larger than unity. The abundance of various topological phases with a large number of protected edge states makes the studied system potentially one of the richest topological materials discovered so far. Since two-dimensional structures in such systems are next in line to be studied experimentally, magnetic adatom structures provide a promising platform for realizing exotic phases of matter of fundamental interest.

Keywords topological matter, topological superconductivity, Majorana modes

ISBN (printed) 978-952-60-6851-0 **ISBN (pdf)** 978-952-60-6852-7

ISSN-L 1799-4934 **ISSN (printed)** 1799-4934 **ISSN (pdf)** 1799-4942

Location of publisher Helsinki **Location of printing** Helsinki **Year** 2016

Pages 90 **urn** http://urn.fi/URN:ISBN:978-952-60-6852-7

A? Aalto-yliopisto

Tiivistelmä

Aalto-yliopisto, PL 11000, 00076 Aalto www.aalto.fi

Tekijä
Joel Röntynen

Väitöskirjan nimi
Topologinen suprajohtavuus magneettisissa atomihiloissa

Julkaisija Perustieteiden korkeakoulu

Yksikkö Teknillisen fysiikan laitos

Sarja Aalto University publication series DOCTORAL DISSERTATIONS 111/2016

Tutkimusala Teoreettinen kondensoituneen aineen fysiikka

Käsikirjoituksen pvm 03.02.2016 **Väitöspäivä** 17.06.2016

Julkaisuluvan myöntämispäivä 16.05.2016 **Kieli** Englanti

☐ **Monografia** ☒ **Artikkeliväitöskirja** ☐ **Esseeväitöskirja**

Tiivistelmä

Topologiset materiaalit ovat viimeisten kolmen vuosikymmenen aikana nousseet yhdeksi aktiivisimmista tutkimuskentistä kondensoituneen aineen fysiikassa. Topologian rooli näiden materiaalien ominaisuuksien määräytymisessä on perustavanlaatuisesti muuttanut ymmärrystämme siitä, miten materian perusosaset järjestyvät tuottaessaan eri aineen olomuotoja. Topologisissa materiaaleissa topologia ilmenee reunatiloina ja eksoottisina kvasihiukkasina, joiden erityislaatuisien ominaisuuksien ennustetaan tuottavan monenlaisia teknologisia sovelluksia.

Tässä väitöskirjassa olen tutkinut topologista suprajohtavuutta, missä ennustetaan esiintyvän lokalisoituneita Majorana-eksitaatioita. Nämä Majorana-kvasihiukkaset rikkovat tavanomaisen jaottelun bosoneihin ja fermioneihin, sillä ne noudattavat niin kutsuttua epäabelista kvanttistatistiikkaa. Täten Majorana-hiukkaset edustavat perustavanlaatuisella tavalla aivan uudenlaista fysiikkaa. Lisäksi Majorana-hiukkasia visioidaan käytettävän topologisesti suojatussa kvanttilaskennassa, millä on toteutuessaan kauaskantoisia vaikutuksia tietojenkäsittelylle. Näistä syistä Majorana-tilojen kokeellinen havaitseminen on eräs ajankohtaisimmista tavoitteista kondensoituneen aineen fysiikassa tällä hetkellä. Tässä väitöskirjassa tutkitut systeemit koostuvat magneettisista atomirakenteista suprajohteen päällä. Julkaisut I ja II käsittelevät lokalisoituneita Majorana-tiloja atomiketjuissa. Julkaisussa I osoitimme muun muassa, että toisiinsa kytkeytyneissä ketjuissa Majorana-tiloja löytyy laajemmalta parametrialueelta kuin erillisissä ketjuissa. Julkaisussa II osoitettiin, että supravirran avulla on mahdollista kontrolloida siirtymää topologisen ja triviaalin faasin välillä.

Julkaisusuissa III ja IV osoitimme, että kaksiulotteiset atomihilat toteuttavat p_x+ip_y-suprajohtavuuden yleistyksen ja siten nämä systeemit ovat mielenkiintoinen lisä epätavanomaisten suprajohteiden listaan. Systeemin mosaiikkimainen faasidiagrammi on seurausta pitkän kantaman elektronihyppäyksestä. Kahdessa ulottuvuudessa Majorana-tilat kulkevat pitkin hilan reunoja ja niiden lukumäärän määrää topologinen invariantti nimeltä Chernin luku. Ennustimme että tyypillisissä materiaaleissa Chernin luku voi olla hyvin suuri. Suurilla Chernin luvuilla varustettujen topologisten faasien runsas määrä asettaa tutkitun systeemin yhdeksi monipuolisimmista tähän mennessä löydetyistä topologisista materiaaleista. Koska kaksiulotteisten atomihilarakenteiden kokeellinen tutkimus on jo suunnitteilla, tutkittu systeemi on lupaava alusta topologisten faasien tutkimukselle.

Avainsanat topologiset materiaalit, topologinen suprajohtavuus, Majorana-tilat

ISBN (painettu) 978-952-60-6851-0 **ISBN (pdf)** 978-952-60-6852-7

ISSN-L 1799-4934 **ISSN (painettu)** 1799-4934 **ISSN (pdf)** 1799-4942

Julkaisupaikka Helsinki **Painopaikka** Helsinki **Vuosi** 2016

Sivumäärä 90 **urn** http://urn.fi/URN:ISBN:978-952-60-6852-7

Preface

The work presented in this thesis was carried out in the Theory of Quantum Matter group of the O.V. Lounasmaa Laboratory, Department of Applied Physics, Aalto University during the years 2013-2016.

I would like to express my gratitude to my advisor D.Tech. Teemu Ojanen for his guidance and support throughout my doctoral studies. His enthusiasm is truly inspiring and his active guidance has been invaluable for the completion of this thesis. I would also like to thank Prof. Pertti Hakonen for all the support he has given.

I would like to acknowledge my fellow group members Alex Weström and Kim Pöyhönen for helpful discussions and the Finnish Cultural Foundation for financial support. I thank my colleagues in the department, Anne-Maria Visuri, David Dasenbrook, Ciprian Padurariu, Kay Brandner, Shuo Mi and Elina Potanina, whose company has made the time here very enjoyable. A special thanks goes to Xavier Albacete, for he has brought much comfort and stability in my life.

Finally, I would like to express my appreciation for my family for their encouragement and support. My father Hannu has always encouraged me in my studies and my mother Margit has made it her priority to take care of the family. I thank my brothers Jere and Jori for encouragement. I am especially grateful to my sister Nelly, whose support has made it easier to go through the tough times in life.

Helsinki, May 29, 2016,

Joel Röntynen

Contents

List of Publications

This thesis consists of an overview and of the following publications which are referred to in the text by their Roman numerals.

I Kim Pöyhönen, Alex Weststrom, Joel Röntynen, and Teemu Ojanen. Majorana states in helical Shiba chains and ladders. *Physical Review B*, 89,115109, March 2014.

II Joel Röntynen and Teemu Ojanen. Tuning topological superconductivity in helical Shiba chains by supercurrent. *Physical Review B*, 90, 180503(R), November 2014.

III Joel Röntynen and Teemu Ojanen. Topological Superconductivity and High Chern Numbers in 2D Ferromagnetic Shiba Lattices. *Physical Review Letters*, 114, 236803, June 2015.

IV Joel Röntynen and Teemu Ojanen. Chern mosaic - topology of chiral superconductivity on ferromagnetic adatom lattices. *Physical Review B*, 93,094521, March 2016.

Author's Contribution

Publication I: "Majorana states in helical Shiba chains and ladders"

The author performed some of the numerical simulations and contributed to the preparation of the manuscript.

Publication II: "Tuning topological superconductivity in helical Shiba chains by supercurrent"

The author carried out the numerical simulations and contributed to the preparation of the manuscript.

Publication III: "Topological Superconductivity and High Chern Numbers in 2D Ferromagnetic Shiba Lattices"

The author contributed to the derivation of the model, performed the numerical simulations and contributed to the preparation of the manuscript.

Publication IV: "Chern mosaic - topology of chiral superconductivity on ferromagnetic adatom lattices"

The author performed the numerical simulations and made the main contribution to the preparation of the manuscript.

1. Introduction

The study of topological phases of matter is an area of immense activity in condensed matter physics at the moment. The prominence of topology in condensed matter stems from the fact that there are phases of matter satisfying the same symmetries but having different physical properties. This observation does not fit in the traditional Landau symmetry breaking classification of phases of matter and thus requires a new classification scheme. The difference in physical properties in such cases are found to be topological in origin.

Topology studies the classification of shapes according to properties that do not vary when the object is stretched, twisted or otherwise continuously deformed. In this sense a coffee cup and a doughnut are equivalent since they have the same topological properties, namely, the number of handles. Topology in the classification of phases matter is not related to the spatial properties of the system, but rather manifests itself more abstractly in the quantum mechanical properties.

Because topological properties are global features, and hence not affected by local perturbations, they are exceptionally robust. One can think of a knot, which is a global feature of a piece of string and therefore cannot be untied by locally poking the knot. For this reason we can expect the topological properties of a physical system to be robust against imperfections and other local perturbations. An example of a robust topological effect is the integer quantum Hall effect, where the conductance is quantized at extreme precision, serving as a standard of resistance. As the topological properties do not depend on microscopic details, the quantization is exact from sample to sample.

Since the identification of topological invariants in the quantum Hall effect [1] and superfluid ^{3}He [2] in 1982, topology has been found to be ubiquitous in condensed matter systems. There is a wealth of materials

known as topological insulators [3, 4]. Topological insulators have a bulk energy gap, but they can host topologically protected conducting surface states. These surface states are immune to local perturbations that preserve the pertinent symmetries, as long as the bulk gap does not close.

Similarly to topological insulators, superconductors and superfluids can be topological too [4, 5]. In this case the energy gap giving the topological robustness is due to superconducting pairing and the surface states are mixtures of particle and hole-like quasi-particles. The particle-hole picture of the fermionic ground state provides an analogy to particles and anti-particles in high-energy physics. Especially interesting is the analogy to a Majorana fermion, a spin-1/2 particle that is its own anti-particle. The condensed matter equivalent of a Majorana fermion is a localized zero-energy excitation called a Majorana bound state. It differs from the Majorana fermion in particle physics and the usual fermionic quasi-particles in condensed matter that obey Fermi-Dirac statistics by having non-Abelian exchange statistics. An exchange of two identical Majorana bound states need not lead to the same state (with a possible phase difference) like in the case of bosons and fermions. Instead, there is a family of degenerate ground-states, which can be reached by exchanging the Majoranas. Crucially, the resulting state may depend on the order of the exchanges performed, making the exchange statistics non-Abelian.

The experimental realization of these exotic particles would be an important achievement in our understanding of the phases of matter. Additionally, the Majorana bound states are believed to have important technological consequences. The non-Abelian statistics are expected to enable topologically protected quantum computing. The development of a quantum computer would bring profound benefits for computational tasks, such as an ability to factor large numbers used in information security and ultra-fast searches of unstructured databases [6]. However, various proposals for quantum computation generally suffer from decoherence, which destroys the quantum behaviour essential for quantum computation. Topologically protected Majorana bound states are not affected by local perturbations and are thus resilient against the detrimental effects of decoherence. Hence a quantum computer based on Majoranas would be fault-tolerant at the hardware level, although achieving a universal quantum computer requires additional implementation of topologically unprotected operations [7].

The first step on the path towards topological quantum computation is

to show that the Majorana bound states do exist in condensed matter systems. There have been various proposals to observe them in solid-state systems in proximity to a conventional superconductor: two-dimensional topological insulator [8, 9] or semiconductor [10, 11] heterostructures, semiconductor wires [12, 13], and magnetic chains [14, 15]. There are also similar proposals for cold gases of fermionic atoms [16, 17]. All these proposals utilize established experimental techniques to engineer the otherwise rare conditions in which topological superconductivity appears. For this reason experiments in this area have quickly developed into an active field of research.

The first experimental signatures of Majorana zero-energy modes were observed in 2012 in the semiconductor nanowire setup as a zero-bias differential conductance peak [18]. The differential conductance probes the density of states at a given energy and here zero-bias means a state at the Fermi level. A zero-bias peak appearing at a finite magnetic field was therefore taken as a signature of a Majorana bound state. Other experiments supporting this view have since followed [19, 20, 21, 22, 23]. In 2014 a different experimental approach using ferromagnetic Fe chains on superconducting Pb produced convincing evidence for the existence of a Majorana bound state [24]. In contrast to the nanowire platform, this setup allows local probing of the density of states with a scanning tunneling microscope. As predicted by theory, the zero-energy states were found to be localized at the end of the chain, while the bulk remained gapped. Subsequent experiments have further supported these findings [25, 26].

The mounting evidence for the existence of Majorana zero modes in solid-state systems, although very convincing, is not yet fully conclusive since there are other mechanisms that could produce similar experimental signatures[1]: [30, 31, 32, 33, 34, 35]. Therefore the Majorana modes in condensed matter have yet remained elusive and extensive efforts are currently made in the condensed matter community to verify its existence.

The research presented in this thesis is related to the second experimental approach, namely magnetic adatom structures on a conventional superconductor. Here we propose novel platforms for topological superconductivity and explore their experimental consequences. In Publications I and II we study Majorana end states in atomic chains and ladders

[1]Maybe the most unambiguous way to eliminate the alternative mechanisms is to directly demonstrate the non-Abelian exchange statistics obeyed by the Majorana bound states. Experiments in this direction are already anticipated [27, 28, 29].

with magnetic helix structures. Publications III and IV extend the one-dimensional structures into two dimensions with ferromagnetic ordering. There we show how such systems may realize an exceptionally rich platform for topological superconductivity.

The structure of this overview is the following. In Chapter 2 we elucidate the properties of the Majorana excitations in condensed matter systems. In Chapter 3 we illustrate the topological properties of superconducting systems by investigating simple toy models in one and two dimensions. In Chapter 4 we motivate the models and some of the assumptions that are used in the Publications of this thesis. There we also show how these models will reduce to the toy models in Chapter 3 under certain conditions. Chapter 5 gives a summary of the key findings of the Publications.

2. Majorana fermions in topological superconductors

In this chapter we introduce the concept of a Majorana fermion and explain how it is related to anyons in condensed matter systems.

2.1 Majorana fermions

Majorana fermions are the only fermionic particles that are expected to be their own antiparticles. The concept of a Majorana fermion originates from particle physics. The Dirac equation describes relativistic spin-1/2 particles and their antiparticles. In 1937 Ettore Majorana discovered that the Dirac equation admits also real solutions describing fermions that are their own antiparticles [36]. These particles are now called Majorana fermions. The concept of a Majorana fermion has had its impact on the physics of neutrinos and dark matter, and more recently in condensed matter. Elementary particles of Majorana type have not been identified so far, although neutrinos are not yet ruled out [37].

Some condensed matter systems are proposed to realize analogues of the Majorana fermion as localized zero-energy excitations. The Majorana excitation in condensed matter systems is an emergent particle-like excitation - a quasiparticle. Quasiparticle excitations are collective motion of electrons and ions that behave like free or weakly-interacting particles. Unlike Majorana fermions in particle physics, these condensed matter counterparts do not obey fermionic exchange statistics but so called non-Abelian exchange statistics. Possible hosts for Majorana excitations are superfluid ^{3}He [38], fractional quantum Hall systems [39], intrinsic topological superconductors [40], engineered topological superconductors [41] and ultracold fermionic gases [16, 17].

2.2 Anyons

Majorana bound states have a property that makes them non-Abelian anyons, giving them a potential for technological applications in quantum computing and information storage. To understand this property we review the concept of anyons here.

In three or more dimensions the spin-statistics theorem asserts that any quantum state of indistinguishable particles has to obey either Bose-Einstein or Fermi-Dirac statistics. This corresponds to a symmetry of a many-body quantum state of indistinguishable particles: an exchange of two indistinguishable bosons (fermions) has to lead to the same state with a phase factor 1 (-1). In two dimensions, however, it is possible that the exchange of indistinguishable particles results in an arbitrary phase factor $e^{i\phi}$, which is an intermediate between -1 and 1. Particles with this property are called anyons. They can be found in fractional quantum Hall states.

The difference in particle exchange statistics between two and three (or more) dimensions[1] has a topological explanation [42]. First we observe that an adiabatic exchange of two particles twice corresponds to adiabatically taking one particle around the other. Assuming that the state is nondegenerate, the adiabatic theorem then states that the final state can differ from the initial state only up to a phase factor, which is the Berry phase. In three dimensions this is topologically equivalent to not moving the particles at all. Therefore the only possible phase factors after a single exchange of indistinguishable particles is 1 and -1. In two dimensions, however, the trajectory of the moving particle cannot be shrunk to a point without crossing the other particle. Therefore a particle exchange can lead to a nontrivial winding, allowing the arbitrary phase factor of anyons.

Anyons can be classified either as Abelian or non-Abelian [43]. Non-Abelian anyons are a generalization of the conventional Abelian anyons described above. In the case of Abelian anyons we assumed that when the positions of indistinguishable particles are fixed, there is only one ground state, so that an adiabatic exchange of identical particles can only lead to a phase factor difference in the quantum states. On the other hand, non-Abelian anyons have a family of degenerate ground states for fixed

[1] Exchange statistics in one dimension is not well defined, because in one dimension it is not possible to interchange two particles without one going through the other.

particle positions that differ by internal quantum numbers. Therefore the adiabatic exchange of particles again leads to a ground state, but the final state does not need be the initial state up to a phase factor. Rather, the effect of the exchange is an unitary transformation acting in the subspace of degenerate ground states given by a matrix-valued phase factor. Performing the interchanges in a different order does not lead to the same state in general, and for this reason these particles are called non-Abelian.

The noncommuting exchange statistics of non-Abelian anyons realize braiding statistics, which can be used to implement quantum algorithms [42]. The advantage of using anyonic quasiparticles to implement quantum computations is their resilience towards decoherence due to the nonlocal properties of these quasiparticles. The nonlocal properties and their topological origin are discussed in the next chapter.

The usual constituents of matter are either bosons or fermions even if they are confined to move in two dimensions. However, the quasiparticle exitations of a many-body system can be anyonic and the system is then topologically nontrivial. A fractional quantum Hall state with a filling factor $\nu = 5/2$ hosts Majorana quasiparticles and was the first physical system theorized to realize non-Abelian statistics [44, 45]. While there are other theoretical proposals, the only system with at least indirect experimental evidence for non-Abelian statistics are fractional quantum Hall states of two-dimensional electron gases [39]. Read and Green [46] established the connection between strongly interacting $\nu = 5/2$ fractional quantum Hall state and a spinless $p + ip$ superconductor in two dimensions, which is a weakly interacting system and has a simple microscopic description. This discovery has led to the current efforts for engineering topological superconductivity.

3. Topological superconductivity

In this chapter we elucidate the topological properties of superconducting systems. We begin by reviewing the concept of the Berry phase, as it plays an important role in the topological classification of materials. To illustrate the emergence of topological superconductivity and its basic properties, we first consider two simple toy models describing spinless fermions on one and two dimensions. In chapter 4 we will show how models describing real physical systems can be reduced to such effective models.

3.1 Berry phase

Let us consider a Hamiltonian $H(\mathbf{R}(t))$ with a set of parameters that change over time, $\mathbf{R}(t) = (R_1(t), R_2(t), \dots)$. A time-dependent Hamiltonian does not have energy eigenstates that evolve according to the time-independent Schrödinger equation, but we can define instantaneous eigenstates $\chi_n(\mathbf{R}(t))$ that are eigenfunctions of the Hamiltonian at a given time t,

$$H(\mathbf{R}(t))\,|\chi_n(\mathbf{R}(t))\rangle = E_n(\mathbf{R}(t))\,|\chi_n(\mathbf{R}(t))\rangle. \tag{3.1}$$

We consider a system that is initially in one of the instantaneous eigenstates, $|\psi(0)\rangle = |\chi_n(\mathbf{R}(0))\rangle$. If the state remains nondegenerate throughout the evolution and the parameters $\mathbf{R}(t)$ change slowly compared to the time scale related to the energy level separation, the quantum adiabatic theorem says that a state starting as an instantaneous eigenstate of the system will evolve into a corresponding instantaneous eigenstate at a later time with a time-dependent phase factor,

$$|\chi_n(\mathbf{R}(t_0))\rangle \to e^{i\phi(t)}|\chi_n(\mathbf{R}(t))\rangle. \tag{3.2}$$

We are interested in cyclic evolution of the system corresponding to loops in the parameter space, $\mathbf{R}(0) = \mathbf{R}(T)$, with a period T. The phase ϕ in Eq. (3.2) consists of the usual dynamical phase

$$\phi_{\rm dyn} = -\frac{1}{\hbar}\int_0^T dt\, E_n(t) \tag{3.3}$$

and the Berry phase

$$\phi_{\rm B} = i\int_0^T dt\, \langle \chi_n(\mathbf{R}(t))|\frac{d}{dt}|\chi_n(\mathbf{R}(t))\rangle. \tag{3.4}$$

Because the instantaneous eigenstates depend on time only through the parameters $\mathbf{R}(t)$, by using the chain rule

$$\frac{d}{dt} = \sum_j \frac{dR_j(t)}{dt}\frac{\partial}{\partial R_j(t)} \tag{3.5}$$

the accumulated Berry phase over a loop C in the parameter space can be expressed as

$$\phi_{\rm B} = \oint_C \mathbf{A}_n(\mathbf{R})\cdot d\mathbf{R}, \tag{3.6}$$

where

$$[\mathbf{A}_n(\mathbf{R})]_j = \langle \chi_n(\mathbf{R})|i\frac{\partial}{\partial R_j}|\chi_n(\mathbf{R})\rangle \tag{3.7}$$

is the Berry connection. The Berry phase depends only on the path C, not on the rate of traversing the path, and therefore it is also called a geometric phase.

The Berry connection is gauge-dependent: under a gauge transformation

$$|\chi_n(\mathbf{R})\rangle \to e^{i\zeta_n(\mathbf{R})}|\chi_n(\mathbf{R})\rangle, \tag{3.8}$$

the Berry connection (3.7) transforms as

$$\mathbf{A}_n(\mathbf{R}) \to \mathbf{A}_n(\mathbf{R}) - \nabla_{\mathbf{R}}\zeta_n(\mathbf{R}). \tag{3.9}$$

Nevertheless, the total Berry phase (3.6) accumulated over a closed path is gauge-independent. By using Stoke's theorem it can be expressed as an integral over a surface S bounded by the loop C. In three dimensions we then have

$$\phi_{\rm B} = \int_S \mathbf{F}_n(\mathbf{R})\cdot d\mathbf{S}, \tag{3.10}$$

where

$$\mathbf{F}_n(\mathbf{R}) = \nabla_{\mathbf{R}}\times\mathbf{A}_n(\mathbf{R}) \tag{3.11}$$

is the Berry curvature vector. In general, the Berry phase is given by an integral of the Berry curvature tensor

$$\mathcal{F}_{jk}^{(n)} = i\left[\left\langle \frac{\partial \chi_n}{\partial_{R_j}} \middle| \frac{\partial \chi_n}{\partial_{R_k}} \right\rangle - \left\langle \frac{\partial \chi_n}{\partial_{R_k}} \middle| \frac{\partial \chi_n}{\partial_{R_j}} \right\rangle\right]. \tag{3.12}$$

over the surface S. Unlike the Berry connection, the Berry curvature is a gauge independent quantity. Here we see a nice analogy to electromagnetism: the Berry connection (3.9) plays the role of the electromagnetic vector potential while the Berry curvature (3.11) is the magnetic field.

In this thesis we are mostly concerned with many-electron systems with two energy bands. Such systems can be described with a Hamiltonian of the general form

$$H(\mathbf{R}) = d_0(\mathbf{R})\mathbb{1}_{2\times 2} + \mathbf{d}(\mathbf{R}) \cdot \boldsymbol{\sigma}, \tag{3.13}$$

where $\boldsymbol{\sigma} = (\sigma_x, \sigma_y, \sigma_z)$ are the Pauli matrices. The Hamiltonian has two eigenvalues,

$$E(\mathbf{R}) = d_0(\mathbf{R}) \pm |\mathbf{d}(\mathbf{R})|, \tag{3.14}$$

and the corresponding eigenvectors depend only on the direction of $\mathbf{d}(\mathbf{R})$. The vector $\mathbf{d}(\mathbf{R})$ is a mapping from the parameter space to the Hilbert space spanned by the eigenstates of the Hamiltonian 3.13. Energy level crossings occur when $\mathbf{d}(\mathbf{R}) = \mathbf{0}$ and the Berry curvature is not well-defined at these points.

As an illustration, let us consider a Hamiltonian of the form

$$\mathbf{d}(\mathbf{R}) = \pm\mathbf{R} \tag{3.15}$$

in three dimensions. There is a level crossing at $\mathbf{R} = \mathbf{0}$. The Berry curvature of the ground state is given by

$$\mathbf{F} = \pm\frac{1}{2}\frac{\mathbf{R}}{|\mathbf{R}|^3} \tag{3.16}$$

in its vector form. Having the property

$$\nabla_{\mathbf{R}} \cdot \mathbf{F} = \pm 2\pi\delta(\mathbf{R}), \tag{3.17}$$

its integral around a surface surrounding the degeneracy point $\mathbf{R} = \mathbf{0}$ is given by

$$\phi_{\mathrm{B}} = \int_S \mathbf{F} \cdot d\mathbf{S} = \pm 2\pi. \tag{3.18}$$

Here we see that the degeneracy point acts as either a source or a sink of the Berry curvature.

To continue the analogy to electromagnetism, we note that the degeneracy points are like magnetic monopoles. A magnetic monopole has always a Dirac string attached to it that carries the 2π-flux to the monopole,

where it spreads radially. The Dirac string appears because there is no continuous single-valued gauge choice for the eigenvectors on the sphere around the monopole. Different gauge choices move the position of the string, but it can never be eliminated. This leads to the quantization of the electric charge. In the same way, the degeneracy points in the parameter space can lead to quantized Berry phase. This happens when, in the course of cyclic adiabatic evolution, $\mathbf{d}(\mathbf{R})$ covers a sphere surrounding a degeneracy point.

3.2 Kitaev chain

We now consider a model for spinless fermions in a chain, which was introduced by Kitaev [47] in 2001 as a prototype for topological superconductivity. The fermions in the chain experience induced superconducting pairing correlations that are described at the mean-field level. The Hamiltonian of the chain of N sites is then given by

$$\hat{H} = \sum_{n=1}^{N-1} \Big[t(\hat{c}_n^\dagger \hat{c}_{n+1} + \hat{c}_{n+1}^\dagger \hat{c}_n) - \mu \hat{c}_n^\dagger \hat{c}_n + \Delta(\hat{c}_{n+1}^\dagger \hat{c}_n^\dagger + \hat{c}_n \hat{c}_{n+1}) \Big], \tag{3.19}$$

where $\hat{c}_n^\dagger$ creates an electron at the atomic site n and $\hat{c}_n$ is the corresponding annihilation operator. The first term describes the nearest-neighbour hopping with an amplitude t and the second term gives the on-site energy in terms of the chemical potential μ. As two identical fermions cannot occupy the same orbital state, there cannot be on-site pairing in the absence of the spin and orbital degrees of freedom. Therefore we consider superconducting pairing between the nearest neighbours. The pairing amplitude $\Delta e^{i\phi}$ has been chosen to be real by performing a gauge transformation $\hat{c}_n \to e^{-i\phi/2}\hat{c}_n$.

To understand the topological properties of the chain, it is instructive to transform into a Majorana basis,

$$\hat{c}_n = \frac{1}{2}(\hat{\gamma}_{A,n} + i\hat{\gamma}_{B,n}), \quad \hat{c}_n^\dagger = \frac{1}{2}(\hat{\gamma}_{A,n} - i\hat{\gamma}_{B,n}), \tag{3.20}$$

which is just a decomposition of the complex fermionic operator $\hat{c}_n$ into its real and imaginary part. The Majorana operators $\hat{\gamma}_{A,n}$ and $\hat{\gamma}_{B,n}$ are real,

$$\hat{\gamma}_{\alpha,n}^\dagger = \hat{\gamma}_{\alpha,n}, \quad \alpha = A, B, \tag{3.21}$$

and satisfy the following anticommutation relation

$$\{\hat{\gamma}_{\alpha,m}, \hat{\gamma}_{\beta,n}\} = 2\delta_{\alpha\beta}\delta_{mn}. \tag{3.22}$$

These relations imply $\hat{\gamma}_{\alpha,n}^{\dagger}\hat{\gamma}_{\alpha,n} = \hat{\gamma}_{\alpha,n}^{2} = 1$ so that there is no meaning in the state $\hat{\gamma}_{\alpha,n}$ being occupied or unoccupied. It is only by pairing two Majorana operators into a fermionic operator, as in Eq. (3.20), that we have a physical state that can be occupied by a (quasi)particle.

The Hamiltonian (3.19) in the Majorana basis is given by

$$\hat{H} = \frac{i}{2}\sum_{n=1}^{N-1}\Big\{(t+\Delta)\hat{\gamma}_{A,n}\hat{\gamma}_{B,n+1} + (t-\Delta)\hat{\gamma}_{A,n+1}\hat{\gamma}_{B,n} - \mu\hat{\gamma}_{A,n}\hat{\gamma}_{B,n}\Big\} \tag{3.23}$$

up to a constant term. In this form of the Hamiltonian we can identify two limiting cases:

(i) For $\Delta = t = 0$ the Hamiltonian (3.23) reduces to

$$\hat{H} = -\frac{\mu}{2}\sum_{n} i\hat{\gamma}_{A,n}\hat{\gamma}_{B,n} = -\mu\sum_{n}\hat{c}_{n}^{\dagger}\hat{c}_{n}, \tag{3.24}$$

which is just the limit of isolated electrons.

(ii) For $\Delta = t$ and $\mu = 0$ we have

$$\hat{H} = t\sum_{n=1}^{N-1} i\hat{\gamma}_{A,n}\hat{\gamma}_{B,n+1}. \tag{3.25}$$

In this limit the Majorana operators of adjacent sites are paired together. We can form new fermionic operators

$$\hat{a}_{n} = \frac{1}{2}(\hat{\gamma}_{A,n} + i\hat{\gamma}_{B,n+1}), \quad \hat{a}_{n}^{\dagger} = \frac{1}{2}(\hat{\gamma}_{A,n} - i\hat{\gamma}_{B,n+1}), \tag{3.26}$$

and Eq. (3.25) is then given by

$$\hat{H} = 2t\sum_{n=1}^{N-1}\hat{a}_{n}^{\dagger}\hat{a}_{n}. \tag{3.27}$$

The Majorana operators $\hat{\gamma}_{B,1}$ and $\hat{\gamma}_{A,N}$ do not appear in the Hamiltonian (3.25), meaning that an electron state formed by pairing the Majorana operators at the chain ends,

$$\hat{a}_{n} = \frac{1}{2}(\hat{\gamma}_{A,N} + i\hat{\gamma}_{B,1}) \tag{3.28}$$

can be occupied without an energy cost. In this limit we can directly see that the system can host highly non-local zero-energy single-fermion state at the chain ends.

The two limiting cases are representatives of two topologically inequivalent parameter regimes. All Hamiltonians that are adiabatically connected to the trivial insulating phase (3.24) are trivial and the Hamiltonians connected to the limit of two unpaired Majorana operators (3.27) are nontrivial. In contrast to the special limit of unpaired Majorana operators

at the opposite ends (3.25), the nontrivial Hamiltonian in general contains all the Majorana operators. There still exists an edge mode whose penetration in the chain decreases exponentially, and whose energy approaches zero exponentially, as the length of the chain increases [47].

3.2.1 Bulk properties

To gain further insight of the transition between the two topologically different regimes, we now consider an infinite chain without boundaries. The discrete translation symmetry of the lattice then allows us to transform into a quasimomentum space by defining a Fourier transform

$$\hat{c}_n = \int_{-\pi/a}^{\pi/a} \frac{dk}{2\pi} e^{ikna} \hat{c}(k), \tag{3.29}$$

where a is the lattice constant. The Hamiltonian (3.19) can then be expressed as

$$\hat{H} = \int_{0}^{\pi/a} \frac{dk}{2\pi} \hat{\Psi}^\dagger(k) \mathcal{H}(k) \hat{\Psi}(k), \tag{3.30}$$

up to a constant term. Here we have introduced the Nambu spinor

$$\hat{\Psi}(k) = \left[\hat{c}(k), \hat{c}^\dagger(-k)\right]^{\mathrm{T}} \tag{3.31}$$

and the Bogoliubov-de Gennes (BdG) Hamiltonian

$$\mathcal{H}(k) = \begin{pmatrix} \epsilon(k) & \tilde{\Delta}(k) \\ \tilde{\Delta}(k)^* & -\epsilon(k) \end{pmatrix}, \tag{3.32}$$

where

$$\begin{aligned} \epsilon(k) &= 2t\cos(ka) - \mu, \\ \tilde{\Delta}(k) &= -2i\Delta e^{i\phi}\sin(ka). \end{aligned} \tag{3.33}$$

Here we have reintroduced the phase ϕ of the induced order parameter Δ. In the absence of spin degree of freedom, the pairing term $\tilde{\Delta}(k)$ vanishes at the symmetric points[1] $ka = 0, \pi$ due to fermionic exchange statistics.

Due to the particle-hole symmetry inherent in the mean-field description of superconductivity, the eigenstates of the BdG Hamiltonian (3.32) come in pairs: an eigenstate

$$\psi(k) = \begin{pmatrix} u(k) \\ v(k) \end{pmatrix} \tag{3.34}$$

[1]The first Brillouin zone, $ka \in (-\pi, \pi]$, is 2π-periodic and therefore it has two symmetric points (points satisfying $ka = -ka$), namely the points $ka = 0$ and $ka = \pi$.

with an eigenvalue $E(k)$ has a corresponding eigenstate $\left[v(-k)^*, u(-k)^*\right]^{\mathrm{T}}$ with an eigenvalue $-E(-k)$. By diagonalizing $\mathcal{H}(k)$, the Hamiltonian (3.30) can be given in its eigenbasis,

$$\hat{H} = \int_0^{\pi/a} \frac{dk}{2\pi} E(k)\hat{a}^\dagger(k)\hat{a}(k) \tag{3.35}$$

with a quasiparticle excitation spectrum

$$E(k) = \sqrt{\left(2t\cos(ka) - \mu\right)^2 + 4|\Delta|^2 \sin^2(ka)}, \tag{3.36}$$

and quasiparticle operators

$$\hat{a}^\dagger(k) = u(k)\hat{c}^\dagger(k) + v(k)\hat{c}(-k). \tag{3.37}$$

In Eq. (3.36) we see that the gap in the spectrum closes when $\mu = \pm|2t|$ and otherwise the spectrum is fully gapped. These gap closings mark a quantum phase transition between topologically trivial and nontrivial regimes, as we will demonstrate below.

3.2.2 Topological phase transition

Let us examine more closely what happens at the topological phase transitions. At the gap closing $\mu = 2t$, where we assume $t > 0$, the gap closes at $k = 0$. Hence when μ is close to $2t$, we can expand the Hamiltonian (3.32) to first order in ka near the point $ka = 0$. This gives us a Dirac-like Hamiltonian

$$\mathcal{H} = m\,\tau_z + 2\Delta e^{i\phi} ka\,\tau_y \tag{3.38}$$

with a mass term $m = 2t - \mu$ and a spectrum

$$E = \pm\sqrt{m^2 + 4|\Delta|^2 (ka)^2}. \tag{3.39}$$

At the phase transition $m = 0$, there are two eigenstates with energies $\pm 2|\Delta|ka$. These are the left and right-moving Majorana modes that are free to propagate in the chain with velocity $v = 2|\Delta|$, since the bulk is no longer gapped.

3.2.3 Topological invariant

The Hamiltonian (3.32) can be expressed as

$$\mathcal{H}(k) = \mathbf{d}(k) \cdot \boldsymbol{\tau}, \tag{3.40}$$

where $\boldsymbol{\tau} = (\tau_x, \tau_y, \tau_z)$ are the Pauli matrices and the components of $\mathbf{d}(k)$ are

$$\begin{aligned} d_z(k) &= 2t\cos(ka) - \mu, \\ d_x(k) &= 2|\Delta|\sin\phi\sin(ka), \\ d_y(k) &= 2|\Delta|\cos\phi\sin(ka). \end{aligned} \tag{3.41}$$

For definiteness, let us focus on the case $t > 0$. The vector $\mathbf{d}(\mathbf{k})$ defines a mapping from the Brillouin zone to the Hilbert space spanned by the eigenvectors of the Hamiltonian. These eigenvectors depend only on the direction of $\mathbf{d}(\mathbf{k})$ and in general we have a mapping from the Brillouin zone to a unit sphere.

In our case, however, the symmetries of the Hamiltonian,

$$\begin{aligned} d_x(-k) &= -d_x(k), \\ d_y(-k) &= -d_y(k), \\ d_z(-k) &= d_z(k), \end{aligned} \tag{3.42}$$

restrict the mapping to a unit circle. If we are in the topologically nontrivial regime, $|\mu| < 2t$, the vector $\mathbf{d}(\mathbf{k})$ encircles the degeneracy point $\mathbf{d} = 0$ that acts either as a source or a sink of the Berry curvature. If the phase of the order parameter ϕ is additionally varied by 2π, $\mathbf{d}(\mathbf{k})$ sweeps a surface surrounding the degeneracy point. This leads to a quantized Berry phase that corresponds to transfer of a charge e from one end of the chain to another. The 2π phase change can be realized experimentally in a Josephson junction or tunneling conductance experiments.

When $\mu = \pm 2t$, $\mathbf{d}(\mathbf{k})$ goes over the degeneracy point either at $k = 0$ ($\mu = 2t$) or at $ka = \pi$ ($\mu = -2t$). At the degeneracy point the gap closing allows a quantum phase transition to the topologically trivial regime, $|\mu| > 2t$, where the mapping $\mathbf{d}(\mathbf{k})$ does not encircle the degeneracy point.

The system belongs to the class D in the topological classification table with a $\mathbb{Z}_2$ topological invariant [48]. Since $d_{x,y}(k) = 0$ at $ka = 0, \pi$, the vector $\mathbf{d}(k)$ encircles the degeneracy point if the sign of d_z is different at these two points. Hence the invariant is given by

$$\nu = \mathrm{sign}\{d_z(0)\}\mathrm{sign}\{d_z(\pi)\}, \tag{3.43}$$

which equals 1 when the system is trivial, and -1 when the system is nontrivial.

3.3 $p_x + ip_y$ superconductivity

After showing how topological superconductivity can appear in one-dimensional system, we are going to investigate topological superconductivity in two dimensions, where a $p_x + ip_y$ superconductor serves as a prototype [49]. Furthermore, Read and Green showed that strongly-interacting fractional quantum Hall states with non-Abelian quasiparticles can be mapped into $p_x + ip_y$ superconductivity [46].

We extend the Kitaev chain (3.19) of spinless fermions to a two-dimensional square lattice,

$$\begin{aligned}\hat{H} = \sum_{mn} \Big\{ & t\Big[\hat{c}^\dagger_{m+1,n}\hat{c}_{m,n} + \text{h.c.}\Big] + t\Big[\hat{c}^\dagger_{m,n+1}\hat{c}_{m,n} + \text{h.c.}\Big] - \mu\, \hat{c}^\dagger_{m,n}\hat{c}_{m,n} \\ & + \Big[\Delta \hat{c}^\dagger_{m+1,n}\hat{c}^\dagger_{m,n} + \text{h.c.}\Big] + \Big[i\Delta \hat{c}^\dagger_{m,n+1}\hat{c}^\dagger_{m,n} + \text{h.c.}\Big] \Big\}\end{aligned} \tag{3.44}$$

Here $\hat{c}^\dagger_{m,n}$ creates an electron at the position $\mathbf{r} = (ma, na)$, where a is the lattice constant, and h.c. stands for the hermitian conjugate of the preceding term. The induced superconducting $p_x + ip_y$-pairing is anisotropic with a phase difference i between the x and y-directions.

As in the one-dimensional model, we again transform into the momentum space of an infinite lattice by performing a Fourier transform over the Brillouin zone,

$$\hat{c}^\dagger_{\mathbf{r}} = \int_{\text{BZ}} \frac{d^2k}{(2\pi)^2} e^{i\mathbf{k}\cdot\mathbf{r}} \hat{c}^\dagger(\mathbf{k}). \tag{3.45}$$

The Hamiltonian (3.44) can then be expressed, up to a constant term, in the BdG form as

$$\hat{H} = \int_0^{\pi/a} \frac{dk_x}{2\pi} \int_{-\pi/a}^{\pi/a} \frac{dk_y}{2\pi} \hat{\Psi}^\dagger(\mathbf{k}) \mathcal{H}(\mathbf{k}) \hat{\Psi}(\mathbf{k}), \tag{3.46}$$

where $\hat{\Psi}(\mathbf{k}) = \big[\hat{c}(\mathbf{k}), \hat{c}^\dagger(-\mathbf{k})\big]^{\text{T}}$ and

$$\mathcal{H}(\mathbf{k}) = \begin{pmatrix} \epsilon(\mathbf{k}) & \tilde{\Delta}(\mathbf{k}) \\ \tilde{\Delta}(\mathbf{k})^* & -\epsilon(\mathbf{k}) \end{pmatrix}, \tag{3.47}$$

with

$$\begin{aligned}\epsilon(\mathbf{k}) &= 2t\cos(k_x a) + 2t\cos(k_y a) - \mu, \\ \tilde{\Delta}(\mathbf{k}) &= 2i|\Delta|\Big[\sin(k_x a) + i\sin(k_y a)\Big].\end{aligned} \tag{3.48}$$

The pairing amplitude $\Delta = |\Delta|e^{i\phi}$ is made real by a gauge transformation $\hat{c}(\mathbf{k}) \to e^{i\phi}\hat{c}(\mathbf{k})$.

The Bogoliubov-de Gennes Hamiltonian in Eq. (3.46) can be given as

$$\mathcal{H}(\mathbf{k}) = \mathbf{d}(\mathbf{k}) \cdot \boldsymbol{\tau}, \tag{3.49}$$

where the components of $\mathbf{d}(\mathbf{k})$ are

$$\begin{aligned} d_x(\mathbf{k}) &= -2|\Delta| \sin(k_y a), \\ d_y(\mathbf{k}) &= -2|\Delta| \sin(k_x a), \\ d_z(\mathbf{k}) &= 2t \cos(k_x a) + 2t \cos(k_y a) - \mu. \end{aligned} \tag{3.50}$$

The number of times a mapping from all momentum values to the unit sphere, given by a unit vector $\hat{\mathbf{d}} = \mathbf{d}/|\mathbf{d}|$, covers the unit sphere is given by the Chern number

$$C = \frac{1}{4\pi} \int d\mathbf{k}\, \hat{\mathbf{d}} \cdot \left(\frac{\partial \hat{\mathbf{d}}}{\partial k_x} \times \frac{\partial \hat{\mathbf{d}}}{\partial k_y} \right). \tag{3.51}$$

The integrand gives the solid angle covered by $\hat{\mathbf{d}}$ when integrated over momentum space. The resulting integer is invariant under smooth deformations of $\hat{\mathbf{d}}$ and its value can change only if the gap closes, making $\hat{\mathbf{d}}$ undefined at some point in momentum space.

4. Magnetic adatom lattices

The spinless toy models introduced in Chapter 3 require unconventional superconductivity, because conventional superconductors pair electrons with opposite spins. The simplest type of superconductors allowing the pairing of electrons of the same spin species are p-wave superconductors. Intrinsic p-wave superconductors have not been found so far, although there are some candidate materials, for instance Sr_2RuO_4. Therefore it is desirable to engineer topological superconductivity using materials readily available in the laboratory.

To produce the effectively spinless regime of the toy models in a system with conventional superconductivity, one needs to lift the spin degeneracy of the electrons without destroying the superconducting pairing. The spin degeneracy can be lifted by a magnetic field, but conventional superconductivity, which pairs electron with opposite spins near the Fermi energy, is suppressed or killed in the presence of magnetism. This problem can be circumvented by combining magnetism with spin-orbit coupling, as will be demonstrated in this chapter.

In this thesis we consider magnetic adatom lattices that can be assembled and probed by a scanning tunneling microscope (STM). It is a well-established technique to use STM to individually place atoms on a superconducting surface. STM can also be used to probe the local density of states of the system. This spatial resolution can be used to verify that the zero-energy states are localised at chain ends.

4.1 Shiba state

A magnetic impurity in an s-wave superconductor binds a subgap state localized near the impurity [50]. This state is called a Yu-Shiba-Rusinov state [51, 52, 53], or Shiba state for brevity. The essential physics is cap-

tured by a simple delta-function impurity potential[1] that couples to the bulk electrons through an exchange interaction,

$$H_{\mathrm{imp}} = -JS\sigma_z\,\delta(\mathbf{r}), \tag{4.1}$$

where J is the strength of the exchange interaction and S the magnitude of the impurity spin, which is chosen to be in the z-direction. We neglect the Kondo screening by treating the impurity spin classically[2], so that the impurity spin acts as a local magnetic field.

A conventional s-wave superconductor is described by the BCS Hamiltonian

$$\hat{H}_{\mathrm{BCS}} = \int_{-\infty}^{\infty} d\mathbf{r}\Big[\sum_{\sigma=\uparrow,\downarrow}\hat{\Psi}^\dagger_\sigma(\mathbf{r})\xi(\mathbf{r})\hat{\Psi}_\sigma(\mathbf{r}) + \Delta_0\hat{\Psi}^\dagger_\uparrow(\mathbf{r})\hat{\Psi}^\dagger_\downarrow(\mathbf{r}) + \Delta_0\hat{\Psi}_\downarrow(\mathbf{r})\hat{\Psi}_\uparrow(\mathbf{r})\Big], \tag{4.2}$$

where $\hat{\Psi}^\dagger_\sigma(\mathbf{r})$ creates an electron with spin σ at a position $\mathbf{r}$. The kinetic energy,

$$\xi(\mathbf{r}) = -\frac{\hbar^2}{2m}\nabla^2 - \mu, \tag{4.3}$$

is measured relative to the Fermi energy μ and Δ_0 is the pairing amplitude. In the absence of impurities, the bulk spectrum is given by

$$E(\mathbf{k}) = \sqrt{\left(\frac{\hbar^2|\mathbf{k}|^2}{2m} - \mu\right)^2 + \Delta_0^2}, \tag{4.4}$$

where $\hbar\mathbf{k}$ is the momentum of the conduction electrons. The spectrum is fully gapped, the gap being Δ_0 at the Fermi level.

Adding the impurity term (4.1) to the Hamiltonian creates a bound state below the superconducting gap with an energy [51, 52, 53]

$$E_0 = \frac{1-\alpha^2}{1+\alpha^2}\Delta_0, \tag{4.5}$$

where $\alpha = \pi JS\mathcal{N}$ and $\mathcal{N}$ is the density of states at the Fermi level of the normal metal. The subgap Shiba state is a spin-polarized Bogoliubov quasiparticle,

$$\hat{a}^\dagger_0(\mathbf{r}) = \begin{cases} u_0(\mathbf{r})\hat{\Psi}^\dagger_\downarrow(\mathbf{r}) + v_0(\mathbf{r})\hat{\Psi}_\uparrow(\mathbf{r}) & \text{for } J<0 \\ u_0(\mathbf{r})\hat{\Psi}^\dagger_\uparrow(\mathbf{r}) + v_0(\mathbf{r})\hat{\Psi}_\downarrow(\mathbf{r}) & \text{for } J>0 \end{cases}. \tag{4.6}$$

[1]The delta-function potential describes the scattering at low temperatures, where the isotropic s-wave scattering dominates.

[2]Mathematically this corresponds to the limit $S\to\infty$ while $J\to 0$, so that JS is finite in Eq. (4.1). In the quantum mechanical treatment of the impurity spin, where the Kondo effect is relevant for antiferromagnetic exchange coupling and the results depend strongly on the value of S, the results are qualitatively the same for the antiferromagnetic coupling, while for ferromagnetic coupling the bound state stays close to the gap edge [54, 55].

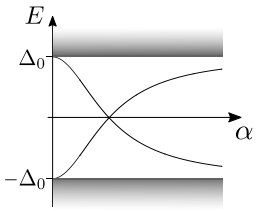

Figure 4.1. The Shiba state energy (4.5) as a function of the coupling strength α. Δ_0 is the induced superconducting gap.

The corresponding time-reversed state is above the gap and does not enter the low-energy description. The Shiba state decays in the bulk with a distance r from the impurity asymptotically as

$$|u_0(\mathbf{r})|, |v_0(\mathbf{r})| \sim e^{-r/\xi_{E_0}}/(k_F r)^{\beta} \tag{4.7}$$

where the exponential cut-off

$$\xi_{E_0} = \frac{\Delta_0}{\sqrt{\Delta_0^2 - E_0}}\,\xi \tag{4.8}$$

is given by the superconducting coherence length ξ for states near the Fermi level, $E_0 \ll \Delta_0$. The power-law decay on the Fermi length scale is given by the parameter β, which is $1/2$ or 1, depending whether the bulk superconductor is two or three-dimensional, respectively.

In the above discussion we have neglected the spatial variation of the order parameter near the magnetic impurity. The bound state is induced because the magnetic moment breaks time-reversal symmetry, leading to a local suppression of the pairing amplitude. Self-consistent calculations reveal that the length scale of the order-parameter variation is determined by the Fermi wavelength [56], which is typically much smaller than the superconducting coherence length.

4.1.1 Quantum phase transition

The bound-state energy as a function of α is illustrated in Fig. 4.1, where the level crossing at $\alpha = \alpha_c$ corresponds to a zero-temperature quantum phase transition [57]. For $\alpha < \alpha_c$, the ground state of the impurity problem is the variational BCS ground state, where all electrons are paired with their time-reversed partner [58]. The first excited state is the BCS ground state with an additional spin-polarized quasiparticle bound to the impurity spin. At the critical coupling, $\alpha_c = 1$, the energy of the bound state crosses the Fermi level and the impurity gap closes. This corresponds to a zero-temperature quantum phase transition [57]. For $\alpha > \alpha_c$,

the two states switch places: now the partially screened impurity spin is the ground state, while the subgap excitation corresponds to removing the bound quasiparticle to create the BCS ground state with an unscreened impurity spin. The crossing is allowed because the two ground states have a different electron parity and different spin quantum number.

The screening of the impurity spin is due to a pair-breaking by the local magnetic field that leads to a local suppression of the pairing potential. Self-consistent mean-field calculations reveal that the spatially varying order parameter acquires a π phase shift, $\Delta \to -\Delta$, near the impurity when the quantum phase transition happens [58]. This is a zero-dimensional topological phase transition and the topological invariant is the ground-state parity. Impurities that can drive a zero-dimensional topological phase transition can in general be used to create nontrivial impurity bands [59]. We already saw that such a band inversion in the Kitaev chain marks a topological phase transition. In section 4.3 we will demonstrate how this band inversion leads to a topological phase transition for a subgap Shiba band.

4.1.2 Scanning tunneling spectroscopy

Scanning tunneling spectroscopy allows probing of the local density of states in the substrate. A bias voltage V between the scanning tunneling microscope (STM) tip and the superconducting substrate allows tunnelling of electrons to a state in the substrate with an energy $E = eV$, where e is the charge of an electron. In a clean bulk superconductor there are no states near the Fermi level due to the spectral gap Δ_0 in Eq. (4.4). Near the impurity, however, the Shiba state (4.6) allows an injection of a spin-down electron or a spin-up hole at an energy $E_0 < |\Delta_0|$. But the injection of a spin-up hole at an energy E_0 just means the extraction of a spin-down electron at an energy $-E_0$, which is achieved by reversing the bias voltage. Therefore the local density of states is given by

$$\rho(\mathbf{r}, E) = |u_0(\mathbf{r})|^2 \delta(E - E_0) + |v_0(\mathbf{r})|^2 \delta(E + E_0) \tag{4.9}$$

and the Shiba state appear as two peaks in the spectral density located symmetrically around the Fermi level. The tunneling intensity is not symmetric with the bias voltage, since the particle and hole amplitudes are normalized as

$$|u_0(\mathbf{r})|^2 + |v_0(\mathbf{r})|^2 = 1. \tag{4.10}$$

For example, if there is a large particle component at a given position, there will be a large peak at a positive bias, while the intensity is low at the negative bias.

4.2 Spin texture

The superconducting pairing that is proximity induced by the underlying superconductor, depends crucially on the orientation of the impurity spins. The impurity spins interact by the Ruderman-Kittel-Kasuya-Yosida (RKKY) interaction mediated by the host superconductor [60, 61, 62], which can lead to ordering of the impurity spins. The presence of spin orbit-coupling on the surface of the superconductor additionally induces the Dzyaloshinsky-Moriya (DM) interaction between the impurity spins [63, 64]. These effects can give rise to a ferromagnetic, antiferromagnetic or helical spin texture [65, 66], but it is not completely clear which type of ordering is favoured under various experimental conditions. There is some experimental evidence for the formation of a spin helix in adatom chains on a normal metal [67, 68] and in nanowires [69]. Ferromagnetic ordering was reported in densely spaced adatom chains [24], where the first signatures of the Majorana end states in the adatom platform were obtained. Helical spin texture was considered in Publications I and II, while in Publications III and IV we assumed a ferromagnetic texture.

4.2.1 Ferromagnatic ordering

If the impurity spins order ferromagnetically, the underlying s-wave pairing correlations that pair together opposite spins cannot be directly induced in the spin-polarized Shiba states. In this case spin-orbit coupling on the surface of the substrate is needed. Inversion symmetry is broken on the surface of the substrate and this can give rise to the Rashba spin-orbit coupling. Electrons moving on the bulk surface feel an effective momentum-dependent magnetic field,

$$H_{\mathrm{Rashba}} = \alpha_{\mathrm{R}}(\boldsymbol{\sigma} \times \mathbf{p}) \cdot \hat{\mathbf{z}}, \tag{4.11}$$

that locks the spin of an electron perpendicular to its momentum. Although spin is no longer a good quantum number, spin-orbit coupling does not break time-reversal symmetry. Hence there are two helical bands,

$$E_{\pm}(\mathbf{k}) = \frac{\hbar^2 k^2}{2m} \pm \alpha_{\mathrm{R}} k - \mu, \tag{4.12}$$

so that electrons moving with an opposite momentum have opposite spins. Hence there is always spin degeneracy at the Fermi level. To achieve the topological regime of effectively spinless fermions, we need to lift this band degeneracy at the Fermi level. A magnetic field perpendicular to the surface will couple the two helicity bands so that the level crossing at $k = 0$ will be gapped. This magnetic field is provided by the ferromagnetic impurity spin texture. If the Fermi level is in the gap, there is only one band at the Fermi level. Furthermore, this band allows pairing between (nearly) time-reversed partners with opposite momentums. This is the mechanism for topological superconductivity in ferromagnetic systems.

4.2.2 Helical ordering

A helical impurity-spin texture, on the other hand, gives rise to a synthetic spin-orbit coupling that can in itself drive the transition to the topological regime. Let us consider a chain of atoms along the x-axis

$$H_{\text{imp}} = -J \sum_n \mathbf{S} \cdot \boldsymbol{\sigma}\, \delta(\mathbf{r} - na\hat{\mathbf{x}}) \tag{4.13}$$

with a spin helix of the form

$$\mathbf{S}_n = (\cos\phi_n \sin\theta, \sin\phi_n \sin\theta, \cos\theta). \tag{4.14}$$

The spins are tilted by an angle θ from the normal of the surface (z-axis) and they rotate in the xy-plane, $\phi_n = n\phi$. We can perform a unitary transformation

$$U(x) = e^{i\sigma_z (x/a)\phi/2} \tag{4.15}$$

to a basis where all the impurity spins are on the same direction, $\mathbf{S}_n = (\sin\theta, 0, \cos\theta)$. The kinetic term of the bulk Hamiltonian (4.2) then acquires an effective spin-orbit-coupling contribution,

$$\xi(\mathbf{r}) = -\frac{\hbar^2}{2m}\left[\left(\partial_x \mp i\phi/(2a)\right)^2 + \partial_y^2\right] - \mu, \tag{4.16}$$

while the pairing terms are unaffected. The magnetic field due to the synthetic spin-orbit coupling is now along the z-axis. As in the case of ferromagnetic texture, a Zeeman-field component perpendicular to the spin-orbit field is needed to open a gap at the crossing between the two helicity bands. For this reason the optimal helical texture for topological superconductivity corresponds to $\theta = \pi/2$. Helical textures are considered in publications I and II. The exact structure of the spin helix in experimental realizations is difficult to predict and therefore the parameters are

treated as variables in the models. It is interesting to note, however, that a helical chain is expected to self-tune to the topological regime due to the back action of the helical texture on the bulk electrons, which would lift the spin degeneracy at the Fermi level [70, 71, 72, 66, 73].

In Publication I we considered Shiba chains with a planar helix. A chain with a planar helix satisfies a chiral symmetry, which is absent in chains with nonplanar helices. The chiral symmetry gives rise to a $\mathbb{Z}$-invariant and the system can have multiple Majorana states at the chain ends and domain walls. Planar spin structures require spin-orbit terms to break the SU(2) spin-rotation symmetry, but these terms also violate the chiral symmetry. For small spin-orbit coupling strengths the chiral symmetry can nevertheless be considered an approximate symmetry. However, in Publication I we do not consider the origin of the spin texture.

4.3 Shiba lattices

Let us consider an array of magnetic adatoms deposited on a superconductor. If the adatoms are sufficiently far apart, the overlap of atomic orbitals is very small and interatomic hopping does not enter the low-energy description. Each adatom however induces a spin-polarized subgap Shiba state due to the local magnetic moment, as illustrated in Fig. 4.2a. The long-range Shiba states can overlap and form a hybridized electronic band inside the superconducting gap (Fig. 4.2b). As the hybridization gets stronger, the bandwidth increases and eventually touches the Fermi level. The induced pairing correlations can then reopen the impurity-band gap, marking a transition to a topological regime (Fig. 4.2c). The induced pairing correlations necessarily have odd pairing symmetry because the Shiba states are spin-polarized.

If the Shiba states lie deep in the gap and the bandwidth due to hybridization is small (see Fig. 4.2c), we can neglect coupling to the states outside the gap at low temperatures [74]. This is the deep-dilute limit considered in Publications II, III and IV. In this limit we can introduce an effective spinless low-energy description

$$\hat{H} = E_0 \sum_n \hat{c}_n^\dagger \hat{c}_n + \sum_{m \neq n} t_{mn} \left[\hat{c}_m^\dagger \hat{c}_n + \hat{c}_n^\dagger \hat{c}_m \right] + \sum_{m \neq n} \Delta_{mn} \left[\hat{c}_m^\dagger \hat{c}_n^\dagger + \hat{c}_n \hat{c}_m \right], \quad (4.17)$$

where $\hat{c}_n^\dagger$ creates a Shiba state at an adatom site n. Here E_0 is the energy of an isolated Shiba state and t_{mn} the hopping amplitude between the Shiba states due to the hybridization, and Δ_{mn} is the induced super-

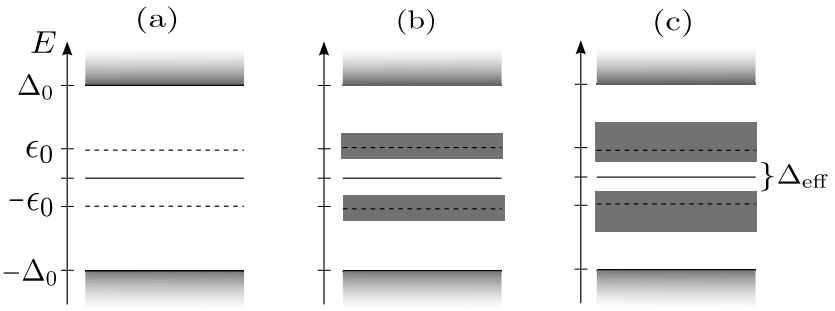

Figure 4.2. Formation of the Shiba band in an array of magnetic impurities on superconductor with a pairing gap Δ_0. (a) The subgap Shiba level ϵ_0 of an isolated impurity. (b) For a small overlap of the Shiba state wave functions, the Shiba states hybridize and form a band around ϵ_0. (c) As the impuritities are brought closer together, the band width increases and eventually touches the Fermi level. The induced pairing correlations can then reopen the effective impurity-band gap, which marks the transition to the topological regime.

conducting pairing. On-site pairing is not allowed, $\Delta_{nn} = 0$, due to the strong exchange interaction at the adatom site. The long-range hopping and pairing amplitudes t_{mn} and Δ_{mn} inherit their asymptotic behaviour,

$$t_{mn}, \Delta_{mn} \sim e^{-r/\xi}/(k_F r)^{\beta}, \tag{4.18}$$

from the Shiba wave functions (4.7). The coherence length of the superconducting substrate ξ gives the length scale for the exponential cut-off, while there is only an algebraic suppression at length scales given by the Fermi wavevector k_F. In typical experimental situations the coherence length is much larger than the Fermi length scale. Both amplitudes have additional sinusoidal oscillations at the Fermi length scale. In publications III and IV we showed that the interplay of these long-range amplitudes leads to intriguingly complex behaviour.

If only nearest-neighbour hopping and pairing are considered, the tight-binding model (4.17) for a chain of Shiba states reduces to the Kitaev chain:

$$\hat{H} = E_0 \sum_n \hat{c}_n^\dagger \hat{c}_n + \sum_n t\left[\hat{c}_n^\dagger \hat{c}_{n+1} + \hat{c}_{n+1}^\dagger \hat{c}_n\right] + \sum_n \Delta\left[\hat{c}_n^\dagger \hat{c}_{n+1}^\dagger + \hat{c}_{n+1}\hat{c}_n\right], \tag{4.19}$$

where the energy of an uncoupled Shiba state, E_0, plays the role of the chemical potential of the Kitaev chain[3]. This can be considered to be the simplest model to simulate the low-energy physics of a Shiba chain. In section 3.2 we learned that the Kitaev chain is topological when the chemical potential is within the bandwidth of the normal state, which translates to $|E_0| < 2|t|$ for the model (4.19). Under this condition the Shiba

[3]The physical chemical potential of the Shiba chain is the Fermi energy in the middle of the gap in the spectrum.

band reaches the Fermi level and the induced pairing correlations can reopen the gap.

In Publication I we adopted a similar model for describing a Shiba chain with a helical magnetic texture. In contrast to the long-range model (4.17), the model for nearest-neighbour hopping (4.19) is more applicable to closely-packed chains where the orbital overlap dominates. This is the case in the epitaxially grown ferromagnetic Fe chains investigated in Refs. [24, 25, 26].

5. Summary of the findings

In Publication I we study chains of atoms with a planar magnetic helix texture. There we show that a magnetic domain wall supports an enhanced zero-bias peak compared to the Majorana modes at the ends of the chain. We also study a ladder structure where atomic chains are coupled to each other. We observe that a ladder structure provides a wider parameter range for topological superconductivity compared to a single chain. Remarkably, the ladder structure can be in the topological regime even when individual chains are trivial.

In Publication II we show that in an atomic chain with helical magnetism, supercurrent can drive the system from a trivial to a topological phase and vice versa. This driving could be applied to move Majorana bound states along the chain, which is needed to demonstrate the non-Abelian statistics.

In Publications III and IV we investigated two-dimensional adatom structures with ferromagnetic ordering. In Publication III we showed that the two-dimensional Shiba lattice produces a long-ranged generalization of a $p_x + ip_y$ superconductor, making it an interesting addition to the list of materials with unconventional pairing. The mosaic-like structure of the topological phase diagram is remarkably rich due to the interplay of hopping amplitudes of different ranges. The number of propagating Majorana modes at the boundary is given by the Chern number, which can be very large in this system. We predicted that the Chern number can reach values of the order of the coherence length of the underlying superconductor in the units of the adatom lattice spacing. The model was motivated by the experiments of one-dimensional atom chains. Since two-dimensional structures in such systems are next in line to be studied experimentally, we have shown that magnetic adatom structures provide a promising platform for realizing exotic phases of matter of fundamental interest.

In publication IV we extend the results of Publication III into different lattice structures and study the complex phase space structure in detail. The abundance of various topological phases with a large number of protected edge states makes the studied system potentially one of the richest topological materials discovered so far.

References

[1] D. J. Thouless, M. Kohmoto, M. P. Nightingale, and M. den Nijs. Quantized hall conductance in a two-dimensional periodic potential. *Phys. Rev. Lett.*, 49:405–408, Aug 1982.

[2] G. E. Volovik and V. P. Mineev. Current in superfluid fermi liquids and the structure of vortex cores. *Zh. Eksp. Teor. Phys.*, 83:1025–1037, September 1982.

[3] M. Z. Hasan and C. L. Kane. *Colloquium* : Topological insulators. *Rev. Mod. Phys.*, 82:3045–3067, Nov 2010.

[4] Xiao-Liang Qi and Shou-Cheng Zhang. Topological insulators and superconductors. *Rev. Mod. Phys.*, 83:1057–1110, Oct 2011.

[5] Martin Leijnse and Karsten Flensberg. Introduction to topological superconductivity and majorana fermions. *Semiconductor Science and Technology*, 27(12):124003, 2012.

[6] Michael A. Nielsen and Isaac L. Chuang. *Quantum Computation and Quantum Information: 10th Anniversary Edition*. Cambridge University Press, New York, NY, USA, 10th edition, 2011.

[7] Martin Leijnse and Karsten Flensberg. Introduction to topological superconductivity and majorana fermions. *Semiconductor Science and Technology*, 27(12):124003, 2012.

[8] Liang Fu and C. L. Kane. Superconducting proximity effect and majorana fermions at the surface of a topological insulator. *Phys. Rev. Lett.*, 100:096407, Mar 2008.

[9] Liang Fu and C. L. Kane. Josephson current and noise at a superconductor/quantum-spin-hall-insulator/superconductor junction. *Phys. Rev. B*, 79:161408, Apr 2009.

[10] Jay D. Sau, Roman M. Lutchyn, Sumanta Tewari, and S. Das Sarma. Generic new platform for topological quantum computation using semiconductor heterostructures. *Phys. Rev. Lett.*, 104:040502, Jan 2010.

[11] Jason Alicea. Majorana fermions in a tunable semiconductor device. *Phys. Rev. B*, 81:125318, Mar 2010.

[12] Roman M. Lutchyn, Jay D. Sau, and S. Das Sarma. Majorana fermions and a topological phase transition in semiconductor-superconductor heterostructures. *Phys. Rev. Lett.*, 105:077001, Aug 2010.

[13] Yuval Oreg, Gil Refael, and Felix von Oppen. Helical liquids and majorana bound states in quantum wires. *Phys. Rev. Lett.*, 105:177002, Oct 2010.

[14] T.-P. Choy, J. M. Edge, A. R. Akhmerov, and C. W. J. Beenakker. Majorana fermions emerging from magnetic nanoparticles on a superconductor without spin-orbit coupling. *Phys. Rev. B*, 84:195442, Nov 2011.

[15] S. Nadj-Perge, I. K. Drozdov, B. A. Bernevig, and Ali Yazdani. Proposal for realizing majorana fermions in chains of magnetic atoms on a superconductor. *Phys. Rev. B*, 88:020407, Jul 2013.

[16] Masatoshi Sato, Yoshiro Takahashi, and Satoshi Fujimoto. Non-abelian topological order in s-wave superfluids of ultracold fermionic atoms. *Phys. Rev. Lett.*, 103:020401, Jul 2009.

[17] Liang Jiang, Takuya Kitagawa, Jason Alicea, A. R. Akhmerov, David Pekker, Gil Refael, J. Ignacio Cirac, Eugene Demler, Mikhail D. Lukin, and Peter Zoller. Majorana fermions in equilibrium and in driven cold-atom quantum wires. *Phys. Rev. Lett.*, 106:220402, Jun 2011.

[18] V. Mourik, K. Zuo, S. M. Frolov, S. R. Plissard, E. P. A. M. Bakkers, and L. P. Kouwenhoven. Signatures of majorana fermions in hybrid superconductor-semiconductor nanowire devices. *Science*, 336(6084):1003–1007, 2012.

[19] Anindya Das, Yuval Ronen, Yonatan Most, Yuval Oreg, Moty Heiblum, and Hadas Shtrikman. Zero-bias peaks and splitting in an al-inas nanowire topological superconductor as a signature of majorana fermions. *Nat Phys*, 8(12):887–895, Dec 2012.

[20] Leonid P. Rokhinson, Xinyu Liu, and Jacek K. Furdyna. The fractional a.c. josephson effect in a semiconductor-superconductor nanowire as a signature of majorana particles. *Nat Phys*, 8(11):795–799, Nov 2012.

[21] M. T. Deng, C. L. Yu, G. Y. Huang, M. Larsson, P. Caroff, and H. Q. Xu. Anomalous zero-bias conductance peak in a nb-insb nanowire-nb hybrid device. *Nano Letters*, 12(12):6414–6419, 2012. PMID: 23181691.

[22] A. D. K. Finck, D. J. Van Harlingen, P. K. Mohseni, K. Jung, and X. Li. Anomalous modulation of a zero-bias peak in a hybrid nanowire-superconductor device. *Phys. Rev. Lett.*, 110:126406, Mar 2013.

[23] H. O. H. Churchill, V. Fatemi, K. Grove-Rasmussen, M. T. Deng, P. Caroff, H. Q. Xu, and C. M. Marcus. Superconductor-nanowire devices from tunneling to the multichannel regime: Zero-bias oscillations and magnetoconductance crossover. *Phys. Rev. B*, 87:241401, Jun 2013.

[24] Stevan Nadj-Perge, Ilya K. Drozdov, Jian Li, Hua Chen, Sangjun Jeon, Jungpil Seo, Allan H. MacDonald, B. Andrei Bernevig, and Ali Yazdani. Observation of majorana fermions in ferromagnetic atomic chains on a superconductor. *Science*, 346(6209):602–607, 2014.

[25] Michael Ruby, Falko Pientka, Yang Peng, Felix von Oppen, Benjamin W. Heinrich, and Katharina J. Franke. End states and subgap structure in proximity-coupled chains of magnetic adatoms. *Phys. Rev. Lett.*, 115:197204, Nov 2015.

[26] J. Klinovaja T. Meier S. Kawai T. Glatzel D. Loss E. Meyer R. Pawlak, M. Kisiel. Probing atomic structure and majorana wavefunctions in mono-atomic fe-chains on superconducting pb-surface. *arXiv:1505.06078*, 2015.

[27] R. V. Mishmash A. Higginbotham J. Danon M. Leijnse T. S. Jespersen J. A. Folk C. M. Marcus K. Flensberg J. Alicea D. Aasen, M. Hell. Milestones toward majorana-based quantum computing. *arXiv:1511.05153*, 2015.

[28] B van Heck, A R Akhmerov, F Hassler, M Burrello, and C W J Beenakker. Coulomb-assisted braiding of majorana fermions in a josephson junction array. *New Journal of Physics*, 14(3):035019, 2012.

[29] T. Hyart, B. van Heck, I. C. Fulga, M. Burrello, A. R. Akhmerov, and C. W. J. Beenakker. Flux-controlled quantum computation with majorana fermions. *Phys. Rev. B*, 88:035121, Jul 2013.

[30] Bertrand I. Halperin Jay D. Sau, Erez Berg. On the possibility of the fractional ac josephson effect in non-topological conventional superconductor-normal-superconductor junctions. *arXiv:1206.4596*, 2012.

[31] Dmitry Bagrets and Alexander Altland. Class d spectral peak in majorana quantum wires. *Phys. Rev. Lett.*, 109:227005, Nov 2012.

[32] Jie Liu, Andrew C. Potter, K. T. Law, and Patrick A. Lee. Zero-bias peaks in the tunneling conductance of spin-orbit-coupled superconducting wires with and without majorana end-states. *Phys. Rev. Lett.*, 109:267002, Dec 2012.

[33] D I Pikulin, J P Dahlhaus, M Wimmer, H Schomerus, and C W J Beenakker. A zero-voltage conductance peak from weak antilocalization in a majorana nanowire. *New Journal of Physics*, 14(12):125011, 2012.

[34] Eduardo J. H. Lee, Xiaocheng Jiang, Ramón Aguado, Georgios Katsaros, Charles M. Lieber, and Silvano De Franceschi. Zero-bias anomaly in a nanowire quantum dot coupled to superconductors. *Phys. Rev. Lett.*, 109:186802, Oct 2012.

[35] Eduardo J. H. Lee, Xiaocheng Jiang, Manuel Houzet, Ramon Aguado, Charles M. Lieber, and Silvano De Franceschi. Spin-resolved andreev levels and parity crossings in hybrid superconductor-semiconductor nanostructures. *Nat Nano*, 9(1):79–84, Jan 2014.

[36] Ettore Majorana. Teoria simmetrica dell'elettrone e del positrone. *Il Nuovo Cimento*, 14(4):171–184, 1937.

[37] Frank T. Avignone, Steven R. Elliott, and Jonathan Engel. Double beta decay, majorana neutrinos, and neutrino mass. *Rev. Mod. Phys.*, 80:481–516, Apr 2008.

[38] G.E. Volovik. *The Universe in a Helium Droplet*. International Series of Monographs on Physics. OUP Oxford, 2009.

[39] R. L. Willett, C. Nayak, K. Shtengel, L. N. Pfeiffer, and K. W. West. Magnetic-field-tuned aharonov-bohm oscillations and evidence for non-abelian anyons at $\nu = 5/2$. *Phys. Rev. Lett.*, 111:186401, Oct 2013.

[40] K. Ishida, H. Mukuda, Y. Kitaoka, K. Asayama, Z. Q. Mao, Y. Mori, and Y. Maeno. Spin-triplet superconductivity in sr2ruo4 identified by 17o knight shift. *Nature*, 396(6712):658–660, Dec 1998.

[41] C.W.J. Beenakker. Search for majorana fermions in superconductors. *Annual Review of Condensed Matter Physics*, 4(1):113–136, 2013.

[42] Chetan Nayak, Steven H. Simon, Ady Stern, Michael Freedman, and Sankar Das Sarma. Non-abelian anyons and topological quantum computation. *Rev. Mod. Phys.*, 80:1083–1159, Sep 2008.

[43] Ady Stern. Anyons and the quantum hall effect - a pedagogical review. *Annals of Physics*, 323(1):204 – 249, 2008. January Special Issue 2008.

[44] R. Willett, J. P. Eisenstein, H. L. Störmer, D. C. Tsui, A. C. Gossard, and J. H. English. Observation of an even-denominator quantum number in the fractional quantum hall effect. *Phys. Rev. Lett.*, 59:1776–1779, Oct 1987.

[45] Gregory Moore and Nicholas Read. Nonabelions in the fractional quantum hall effect. *Nuclear Physics B*, 360(2-3):362 – 396, 1991.

[46] N. Read and Dmitry Green. Paired states of fermions in two dimensions with breaking of parity and time-reversal symmetries and the fractional quantum hall effect. *Phys. Rev. B*, 61:10267–10297, Apr 2000.

[47] A Yu Kitaev. Unpaired majorana fermions in quantum wires. *Physics-Uspekhi*, 44(10S):131, 2001.

[48] Andreas P. Schnyder, Shinsei Ryu, Akira Furusaki, and Andreas W. W. Ludwig. Classification of topological insulators and superconductors in three spatial dimensions. *Phys. Rev. B*, 78:195125, Nov 2008.

[49] G.E. Volovik. Quantized hall effect in superfluid helium-3 film. *Physics Letters A*, 128(5):277 – 279, 1988.

[50] A. V. Balatsky, I. Vekhter, and Jian-Xin Zhu. Impurity-induced states in conventional and unconventional superconductors. *Rev. Mod. Phys.*, 78:373–433, May 2006.

[51] Yu L. Bound state in superconductors with paramagnetic impurities. *Acta Physica Sinica*, 21(1):75–91, 1965.

[52] Hiroyuki Shiba. Classical spins in superconductors. *Progress of Theoretical Physics*, 40(3):435–451, 1968.

[53] A. I. Rusinov. On the theory of gapless superconductivity in alloys containing paramagnetic impurities. *JETP*, 29(6):1101–1106, December 1969.

[54] Koji Satori, Hiroyuki Shiba, Osamu Sakai, and Yukihiro Shimizu. Numerical renormalization group study of magnetic impurities in superconductors. *Journal of the Physical Society of Japan*, 61(9):3239–3254, 1992.

[55] Osamu Sakai, Yukihiro Shimizu, Hiroyuki Shiba, and Koji Satori. Numerical renormalization group study of magnetic impurities in superconductors. ii. dynamical excitation spectra and spatial variation of the order parameter. *Journal of the Physical Society of Japan*, 62(9):3181–3197, 1993.

[56] P. Schlottmann. Spatial variations of the order parameter in superconductors containing a magnetic impurity. *Phys. Rev. B*, 13:1–7, Jan 1976.

[57] Akio Sakurai. Comments on superconductors with magnetic impurities. *Progress of Theoretical Physics*, 44(6):1472–1476, 1970.

[58] M. I. Salkola, A. V. Balatsky, and J. R. Schrieffer. Spectral properties of quasiparticle excitations induced by magnetic moments in superconductors. *Phys. Rev. B*, 55:12648–12661, May 1997.

[59] Lukas Kimme and Timo Hyart. Existence of zero-energy impurity states in different classes of topological insulators and superconductors and their relation to topological phase transitions. *Phys. Rev. B*, 93:035134, Jan 2016.

[60] M. A. Ruderman and C. Kittel. Indirect exchange coupling of nuclear magnetic moments by conduction electrons. *Phys. Rev.*, 96:99–102, Oct 1954.

[61] Tadao Kasuya. A theory of metallic ferro- and antiferromagnetism on zener's model. *Progress of Theoretical Physics*, 16(1):45–57, 1956.

[62] Kei Yosida. Magnetic properties of cu-mn alloys. *Phys. Rev.*, 106:893–898, Jun 1957.

[63] I. Dzyaloshinsky. A thermodynamic theory of weak ferromagnetism of antiferromagnetics. *Journal of Physics and Chemistry of Solids*, 4(4):241 – 255, 1958.

[64] Tôru Moriya. Anisotropic superexchange interaction and weak ferromagnetism. *Phys. Rev.*, 120:91–98, Oct 1960.

[65] Andreas Heimes, Daniel Mendler, and Panagiotis Kotetes. Interplay of topological phases in magnetic adatom-chains on top of a rashba superconducting surface. *New Journal of Physics*, 17(2):023051, 2015.

[66] Younghyun Kim, Meng Cheng, Bela Bauer, Roman M. Lutchyn, and S. Das Sarma. Helical order in one-dimensional magnetic atom chains and possible emergence of majorana bound states. *Phys. Rev. B*, 90:060401, Aug 2014.

[67] Matthias Menzel, Yuriy Mokrousov, Robert Wieser, Jessica E. Bickel, Elena Vedmedenko, Stefan Blügel, Stefan Heinze, Kirsten von Bergmann, André Kubetzka, and Roland Wiesendanger. Information transfer by vector spin chirality in finite magnetic chains. *Phys. Rev. Lett.*, 108:197204, May 2012.

[68] Matthias Menzel, André Kubetzka, Kirsten von Bergmann, and Roland Wiesendanger. Parity effects in 120° spin spirals. *Phys. Rev. Lett.*, 112:047204, Jan 2014.

[69] C. P. Scheller, T.-M. Liu, G. Barak, A. Yacoby, L. N. Pfeiffer, K. W. West, and D. M. Zumbühl. Possible evidence for helical nuclear spin order in gaas quantum wires. *Phys. Rev. Lett.*, 112:066801, Feb 2014.

[70] M. M. Vazifeh and M. Franz. Self-organized topological state with majorana fermions. *Phys. Rev. Lett.*, 111:206802, Nov 2013.

[71] Jelena Klinovaja, Peter Stano, Ali Yazdani, and Daniel Loss. Topological superconductivity and majorana fermions in rkky systems. *Phys. Rev. Lett.*, 111:186805, Nov 2013.

[72] Bernd Braunecker and Pascal Simon. Interplay between classical magnetic moments and superconductivity in quantum one-dimensional conductors: Toward a self-sustained topological majorana phase. *Phys. Rev. Lett.*, 111:147202, Oct 2013.

[73] M. H. Christensen B. M. Andersen J. Paaske M. Schecter, K. Flensberg. Self-organized topological superconductivity in a yu-shiba-rusinov chain. *arXiv:1509.07399*, 2015.

[74] Falko Pientka, Leonid I. Glazman, and Felix von Oppen. Topological superconducting phase in helical shiba chains. *Phys. Rev. B*, 88:155420, Oct 2013.

Aalto-DD 111/2016

ISBN 978-952-60-6851-0 (printed)
ISBN 978-952-60-6852-7 (pdf)
ISSN-L 1799-4934
ISSN 1799-4934 (printed)
ISSN 1799-4942 (pdf)

Aalto University
School of Science
Department of Applyied Physics
www.aalto.fi

BUSINESS +
ECONOMY

ART +
DESIGN +
ARCHITECTURE

SCIENCE +
TECHNOLOGY

CROSSOVER

**DOCTORAL
DISSERTATIONS**